The effect of B-site order-disorder in the structure and magnetism of the new perovskite family $La_2MnB'O_6$ with B' = Ti, Zr and Hf

Diana M. Arciniegas Jaimes[a,#], Juan M. De Paoli[a,f], Vivian Nassif[b], Paula G. Bercoff[c,f], Germán Tirao[c,f], Raúl E. Carbonio[a,f] and Fernando Pomiro[d,a *]

[a] *INFIQC (CONICET – Universidad Nacional de Córdoba), Departamento de Fisicoquímica, Facultad de Ciencias Químicas, Universidad Nacional de Córdoba, Haya de la Torre esq. Medina Allende, Ciudad Universitaria, X5000HUA Córdoba, Argentina.*
[b] *UGA, CNRS, Institut Néel, 38000 Grenoble, France.*
[c] *IFEG CONICET, Facultad de Matemática, Astronomía, Física y Computación, Universidad Nacional de Córdoba, Av. Medina Allende s/n, 5000, Córdoba, Argentina.*
[d] *Department of Chemistry, University of Warwick, Gibbet Hill, Coventry, CV4 7AL, United Kingdom.*
[f] *Researchers of CONICET.*

Keywords: Perovskites, Neutron powder diffraction, Anti-site disorder effects, Symmetry-adapted refinements, Magnetic structures, Antiferromangnetism, Spin-glass.

* Corresponding author
e-mail: fpomiro@fcq.unc.edu.ar (F. Pomiro)
#Current affiliation: *IFEG CONICET, Facultad de Matemática, Astronomía, Física y Computación, Universidad Nacional de Córdoba, Av. Medina Allende s/n, 5000, Córdoba, Argentina.*

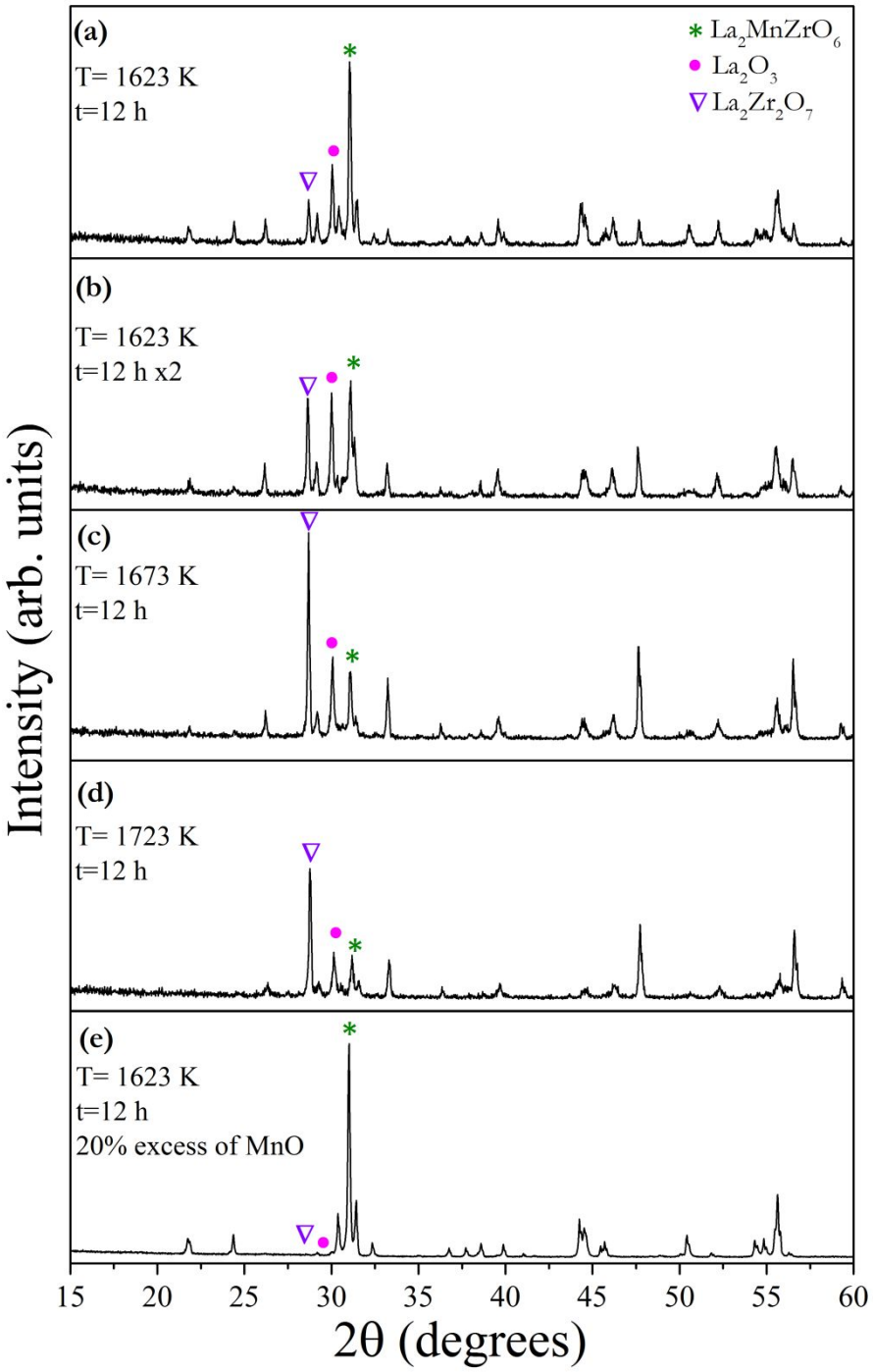

Figure S1: X-ray powder diffraction (XRPD) patterns for different syntheses conditions to obtain the Zr-based perovskite. The conditions used for the syntheses performed with stoichiometric quantities of the regents were: **(a)** 1623 K during 12 h, **(b)** same sample as (a) heated again to the same temperature for 12 h more, **(c)** 1673 K during 12 h and **(d)** 1723 K during 12 h. **e)** Synthesis performed with 20% MnO excess at 1623K during 12 h. The impurities obtained are marked with symbols.

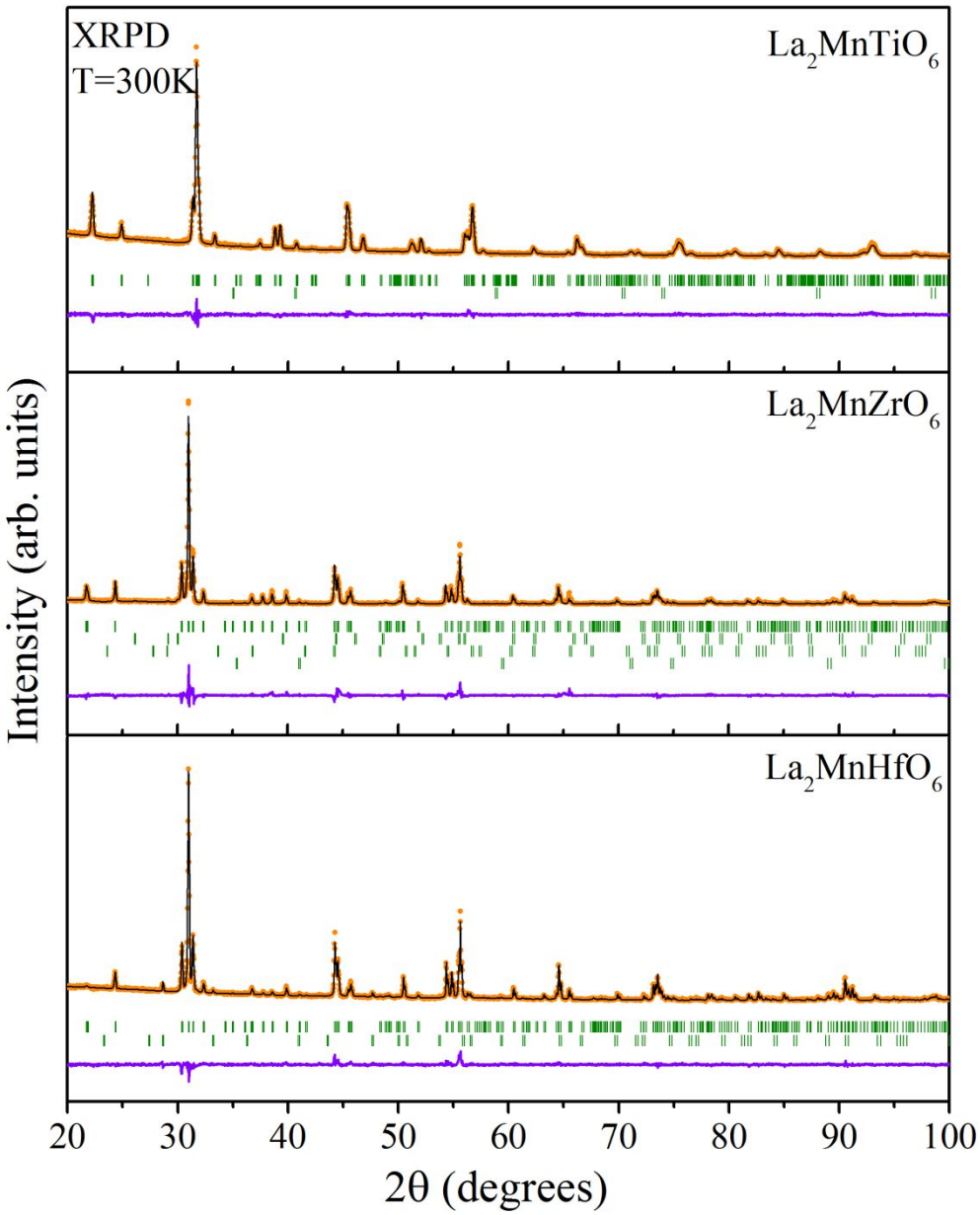

Figure S2: Refined XRPD patterns collected at 300K for B'= Ti, Zr and Hf. Observed (orange dots), calculated (black full line), Bragg reflections (vertical green bars) and difference (violet bottom line). The first set of Bragg reflections corresponds to the main perovskite phase. The second phase for the Ti-based perovskite corresponds to unreacted MnO. For the Zr-based perovskite, the second, third and fourth reflections correspond to La_2O_3, $La_2Zr_2O_7$ and MnO, respectively. For the Hf-based perovskite the second reflections correspond to $La_2Hf_2O_7$. The MnO phase in B' = Zr and Ti was added to the refinements of the XRPD patterns after the detection of this phase in the neutron powder diffraction (NPD) data collected at low temperature, as it is explained in the main text.

Table S1. Atomic coordinates, thermal parameters and occupancies for the whole family of perovskites after Rietveld refinement from NPD data at 300 K. The abbreviation *Occ* indicates the occupation of each crystallographic site in the unit cell.

B'	Space group	Ion	*Site*	*x*	*y*	*z*	B_{iso} (Å^2)	*Occ*
Ti	$P2_1/n$	La	4*e*	0.01086(1)	0.04464(2)	0.24936 (2)	0.46(2)	0.98(1)
		Mn/Ti	2c	0.5	0	0.5	0.17(3)	0.01(1)/0.99 (1)
		Mn/Ti	2b	0.5	0	0	0.45(3)	0.99 (1)/0.01 (1)
		O1	4e	0.30566 (1)	0.71847 (2)	0.04854 (1)	0.74(2)	0.999(1)
		O2	4e	0.71768(2)	0.30672(2)	0.54168(1)	0.74(2)	0.999(1)
		O3	4e	-0.08598(1)	0.52287(1)	0.26037(2)	0.74(2)	0.976(1)
Zr	*Pbnm*	La	4*c*	0.01053(3)	-0.05198(2)	0.25	1.13(2)	0.99(1)
		Mn/Zr	*4b*	0.5	0	0	1.99(2)	0.52(1)/0.48(1)
		O1	*8d*	0.69865(2)	0.30086(2)	-0.05315(2)	0.92(2)	0.99(1)
		O2	*4c*	0.89920(3)	0.53694(3)	0.25	0.92(2)	0.99(1)
Hf	*Pbnm*	La	4*c*	0.01223(1)	-0.05416(2)	0.25	1.02(2)	0.98(1)
		Mn/Hf	*4b*	0.5	0	0	1.19(4)	0.51(1)/0.49(1)
		O1	*8d*	0.69994(3)	0.29929(4)	-0.05302(2)	1.15(2)	0.99(1)
		O2	*4c*	0.89974(2)	0.53237(3)	0.25	1.15(2)	0.99(1)

Table S2. Comparison of the Irreps's notation with the different settings for the high symmetry perovskite parent structure.

A 1*b* (½ ½ ½) B 1*a* (0 0 0) X *3d* (½ 0 0)	**A 1*a* (0 0 0) B 1*b* (½ ½ ½) X *3c* (0 ½ ½)**
R_5^+ - La(a)	**R_4^- - La(a)**
R_5^+ - La(b)	R_4^- - La(b)
X_5^+ - La	**X_5^- - La**
R_5^+ - O(a)	R_4^- - O(a)
R_5^+ - O(b)	R_4^- - O(b)
X_5^+ - O	**X_5^- - O**
R_1^+ - O	**R_2^- - O**
R_4^+ - O	**R_5^- - O**
M_3^+ - O	**M_2^+ - O**
R_3^+ - O	R_3^- - O
M_2^+ - O	M_3^+ - O
M_5^+ - O	M_5^+ - O

Table S3. Refined bond distances B/B'-O, angles (θ) B-O-B' and tilt angles (δ) at RT for the whole family of perovskites. For B'= Zr and Hf: *Site1*=*Site2*= Wyckoff site *4b*. For B'= Ti: *Site1* and *Site2* are *2b* and *2c* Wyckoff sites respectively. The tilting angle of the octahedrons were calculated as δ= (180-θ)/2.

B'		Distances (Å) $(B/B')_{site1}$-O	$(B/B')_{site2}$-O	*θ* (°)	*δ* (°)
Ti	O1	1.978(3) x2	2.155(3) x2	150.7(1)	14.6
	O2	1.958(3) x2	2.159(3) x2	152.6(1)	13.7
	O3	1.975(5) x2	2.134(5) x2	151.8(2)	14.1
	Average	1.9703	2.149	151.7	14.1
Zr	O1	2.122(3)x4		147.25(2)	16.37
	O2	2.123(4)x2		146.40(1)	16.80
	Average	2.122		146.83	16.59
Hf	O1	2.122(3)x4		147.70(2)	16.15
	O2	2.121(4)x2		147.02(2)	16.49
	Average	2.122		147.36	16.32

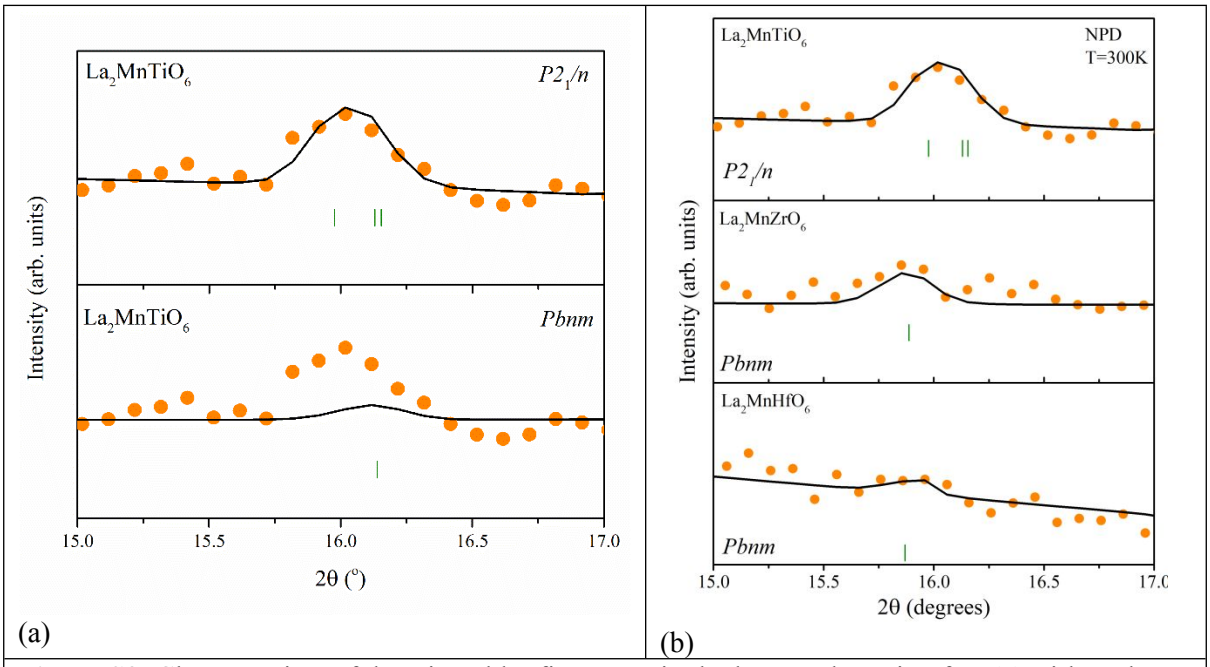

Figure S3: Close-up view of the Rietveld refinements in the low-angle region for: **(a)** Ti-based perovskite with $P2_1/n$ and *Pbnm* models and **(b)** all the studied compounds.

The measured spectra with normalized intensity are shown in **Figure S4a**, where it can be seen that the Kβ' intensity decreases, indicating that the oxidation state of Mn increases, in agreement with previous reports.[1] The fitting obtained is displayed in **Figure S4b**. In order to

quantify the oxidation state of Mn, the intensity Kβ' relative to the total intensity of the Kβ region (I-Kβ') was used. From the corresponding fittings, the oxidation state of Mn for the perovskite was determined by considering the linear fit displayed in **Figure S4c**. From this analysis, it was obtained that the average oxidation state of Mn in the perovskite $La_{0.99(1)}Mn_{0.52(1)}Zr_{0.48(1)}O_{3.00}$ is (2.10 ± 0.11), which is in very good agreement with the value obtained from the analysis of NPD data.

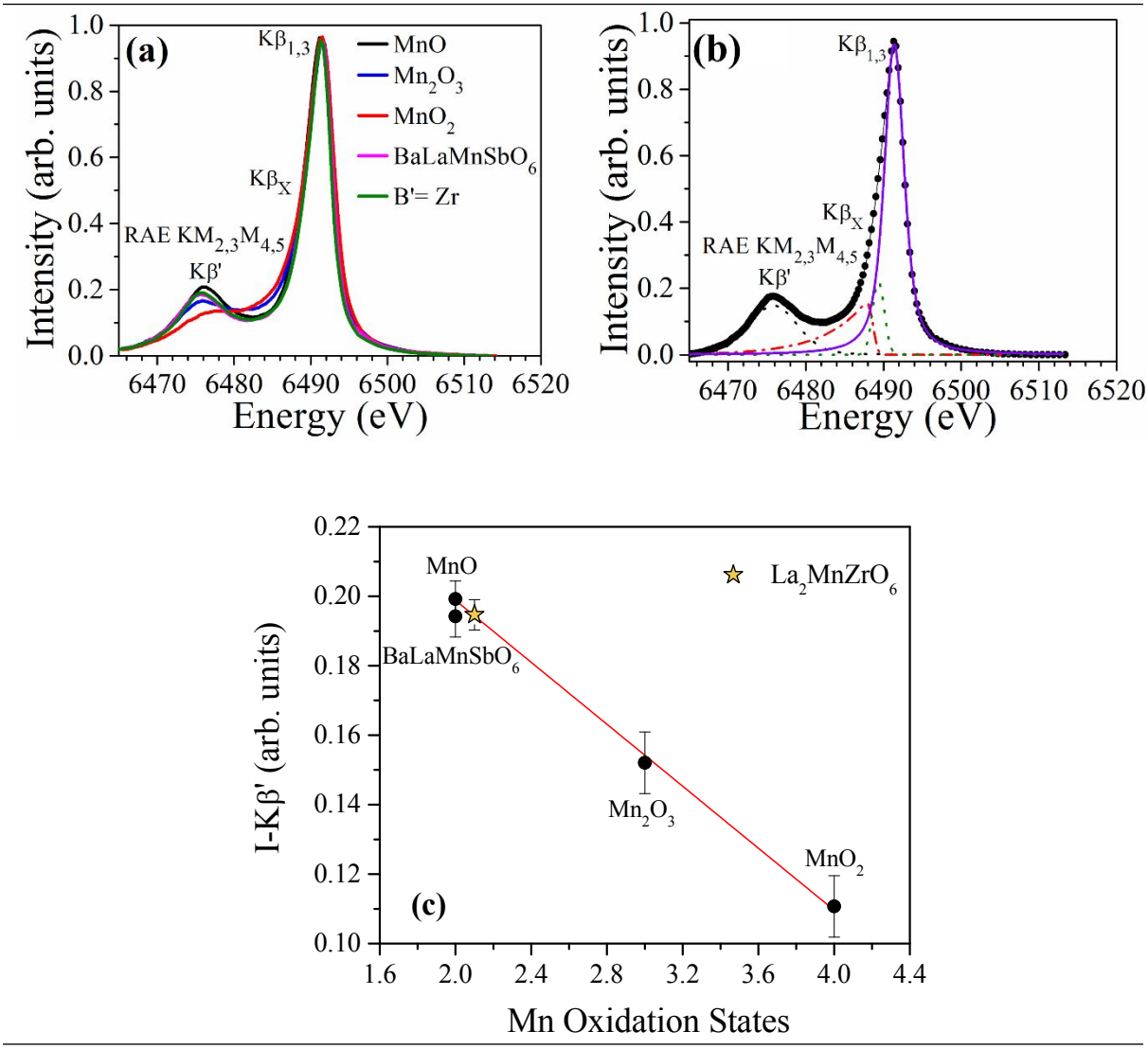

Figure S4: **(a)** Kβ' emission spectra for La_2MnZrO_6 together with the spectra for the Mn reference samples. **(b)** Experimental spectra with the respective fit for B'= Zr. Dots: experimental data; continuous and dotted lines: fitted curve and the corresponding individual contributions of the Voigt functions (Kβ', $K\beta_X$ and $K\beta_{1,3}$ peaks) and EMG (RAE $KM_{2,3}M_{4,5}$ transition). **(c)** Intensity of the Kβ' (I- Kβ') line as a function of the oxidation states of the Mn for the prepared perovskite with B'= Zr.

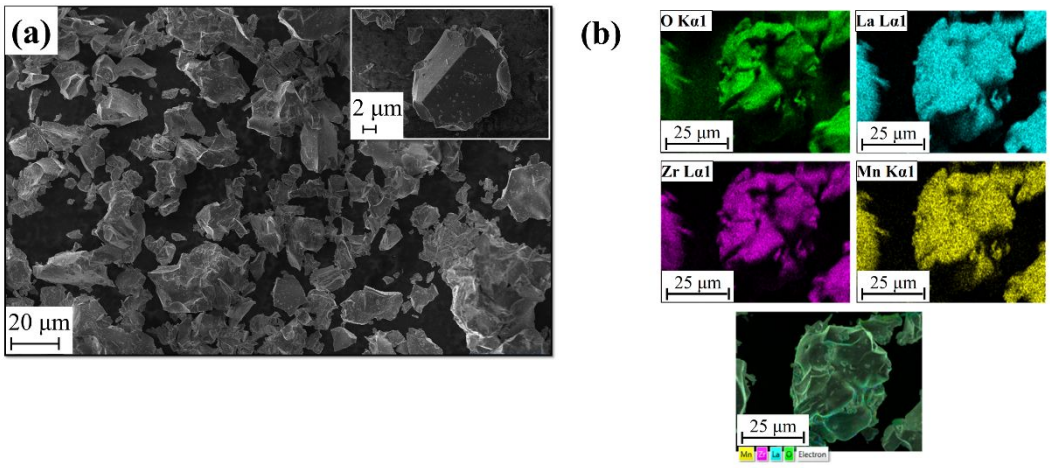

Figure S5: La_2MnZrO_6 shown as a representative example for the whole family **(a)** Scanning electron microscopy images and **(b)** Elemental EDS maps.

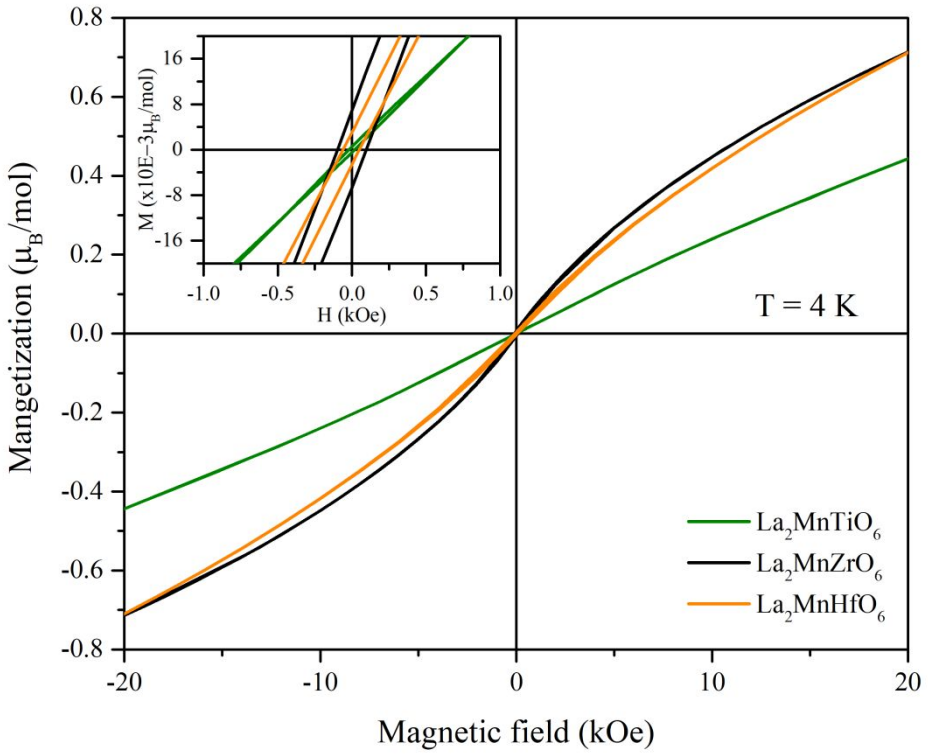

Figure S6: M vs H hysteresis loops for $La_2MnB'O_6$ (B'= Ti, Zr and Hf) measured at 4 K. The inset is a close-up view of the low-field region.

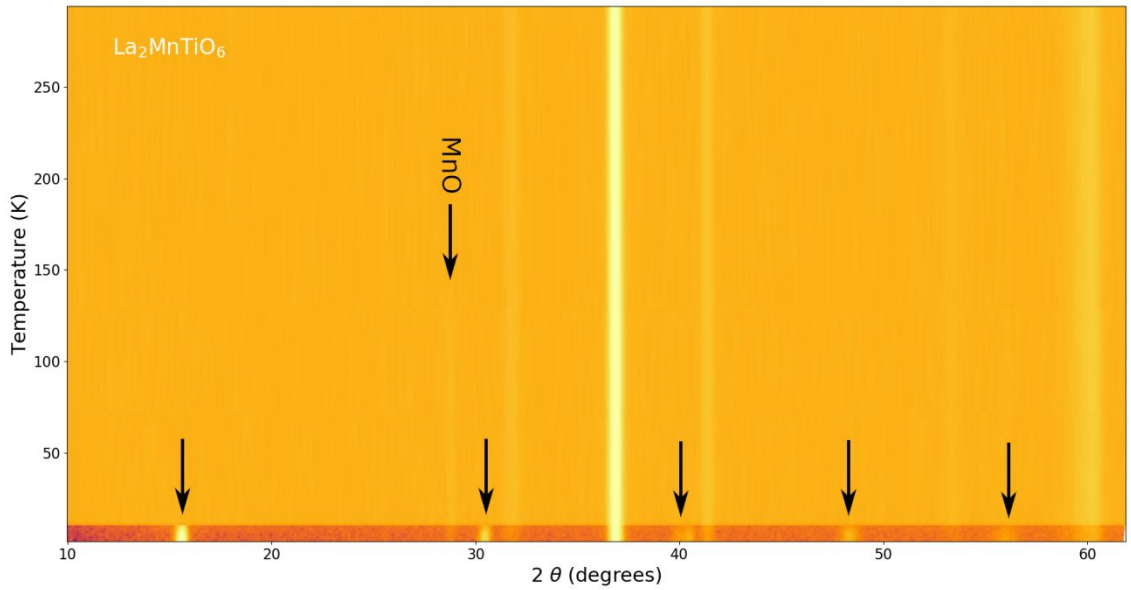

Figure S7: Heat map of NPD data for the Ti-based perovskite. The arrows correspond to the peaks of the magnetic phase.

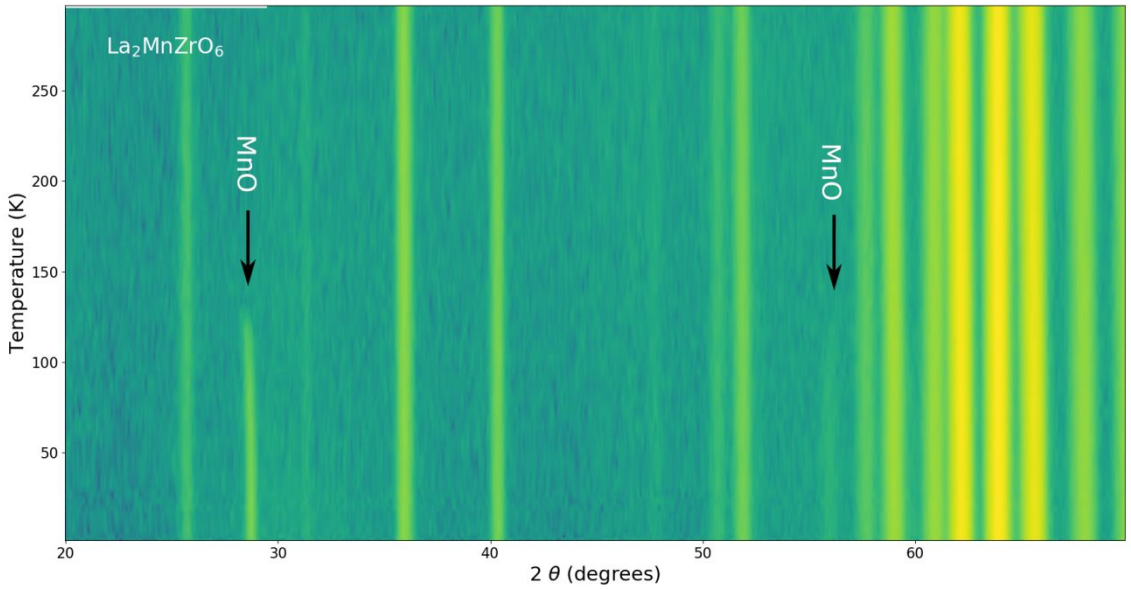

Figure S8: Heat map of NPD data for Zr-based perovskite. The arrows correspond to the magnetic reflections of the unreacted MnO.

Table S4: Crystallographic Data (Powder)			
Source (laboratory X-ray, synchrotron, neutron time of flight (TOF), neutron constant wavelength)	Neutron powder constant wavelength	Neutron powder constant wavelength	Neutron powder constant wavelength
Chemical formula	La_2MnTiO_6	La_2MnZrO_6	La_2MnHfO_6
Formula Weight (g/mol)	476.60	519.92	607.19

Temperature (K)	300	300	300
Pressure (if not ambient)	Ambient	Ambient	Ambient
Wavelength for constant wavelength (NPD) (Å)	1.28	1.28	1.28
Crystal system	Monoclinic	Orthorhombic	Orthorhombic
Space group (No.)	14	62	62
a, b, c, α, β, γ	5.6130(3) 5.7006(3) 7.9724(5) 90.0 89.93(1) 90.0	5.6930(3) 5.8831(3) 8.1313(5) 90.0 90.0 90.0	5.6992(3) 5.8799(3) 8.1381(4) 90.0 90.0 90.0
V (Å^3)	255.10(3)	272.34(3)	272.71(4)
Z	2	4	4
d-space range (Å)	0.80-6.0	0.80-6.0	0.80-6.0
χ^2 (NPD)	47.12	57.55	49.31
R_p (NPD)	7.01	6.06	6.82
R_{wp} (NPD)	6.59	6.60	6.32
Definition of R factors			
$\chi^2=(1/N)\Sigma_i(y_{C,i}-y_{O,i})^2/\sigma^2[y_{O,i}]$			
$R_{wp}^2=\Sigma_i w_i(y_{C,i}-y_{O,i})^2/\Sigma_i w_i(y_{O,i})^2$			

(1) Tsutsumi, K.; Nakamori, H.; Ichikawa, K. X-ray Mn Kb emission spectra of Manganese oxides and manganates. *Phys. Rev. B* **1976,** 13, 929-933.